

## Poly(*N*-isopropyl acrylamide)–Gold Nanoassemblies on Macroscopic Surfaces: Fabrication, Characterization, and Application

Smrati Gupta,<sup>\*,†</sup> Mukesh Agrawal, Petra Uhlmann, Frank Simon, and Manfred Stamm\*

Leibniz-Institut für Polymerforschung Dresden e.V., Hohe Strasse 6, 01069 Dresden, Germany.

<sup>†</sup>Current address: Technische Universität Dresden, Makromolekulare Chemie, Zellescher Weg 19, 01069 Dresden, Germany.

Received October 10, 2009. Revised Manuscript Received November 24, 2009

In this study, we report on the fabrication of the nanoassemblies consisting of the poly(*N*-isopropyl acrylamide) (PNIPAAm) brushes immobilized with gold nanoparticles (Au NPs). The employed process involves grafting of the carboxyl terminated PNIPAAm chains on an underlying substrate in a brush conformation followed by the immobilization of surface functionalized Au NPs by means of physical interaction (hydrogen bonding). Atomic force microscopy (AFM), X-ray photoelectron spectroscopy (XPS), and UV–vis spectroscopy have been employed to characterize the prepared PNIPAAm–Au nanoassemblies. Polymer brushes have been found to suppress the nanoparticles' aggregation and, hence, facilitate the complete surface coverage. Furthermore, we demonstrated the application of resulting PNIPAAm–Au nanoassemblies in the fabrication of the temperature nanosensors. The employed approach is simple and highly versatile for the modification of macroscopic surfaces with a wide range of NPs.

### Introduction

Metal nanoparticles (NPs) represent a special class of the materials, which has recently attracted much attention of the researchers because of their fascinating properties and potential applications in a wide range of areas including in the fabrication of nanosensors, catalysts, electronics, and optical and magnetic devices.<sup>1,2</sup> Earlier studies reveal that the most prominent challenge in dealing with nanoscale particles is to prevent their aggregation in the media.<sup>2</sup> Due to the high surface energy, they tend to aggregate, and aggregation limits their use in above-mentioned applications. A great deal of efforts has been devoted to the stabilization of NPs by exploiting a wide range of stabilizers such as self-assembled monolayers,<sup>3</sup> polymer brushes,<sup>4</sup> dendrimers,<sup>5</sup> latex

particles,<sup>6</sup> microgels,<sup>7</sup> and so on.<sup>8</sup> Among these systems, polymer brushes have been found to offer an easy and effective way for the stabilization of NPs on macroscopic surfaces. Polymer brushes are the assemblies of macromolecules that are tethered by one end to the underlined substrate in such a way that the distance between two grafted chains is lower than that of the radius of the gyration of a polymer chain.<sup>9</sup> Recently, a lot of research has been done on the stabilization of NPs by exploiting the planar and spherical polyelectrolyte brushes.<sup>10</sup> Earlier studies demonstrate that polymer brushes serve as a perfect template for the preparation, stabilization, and application of NPs on the account of their nanometer dimensions, well-defined structure, and ability to control assembly of NPs over multiple length scales, superior precision over template architecture, and the availability of a greater variety of functional groups.<sup>11</sup>

Recently, a great deal of the research efforts have been devoted to the gold (Au) NPs owing to their unique optical properties.<sup>12</sup> In addition, many attempts have

\*To whom correspondence should be addressed. E-mail: smrati.gupta@chemie.tu-dresden.de (S.G.); stamm@ipfdd.de (M.S.).

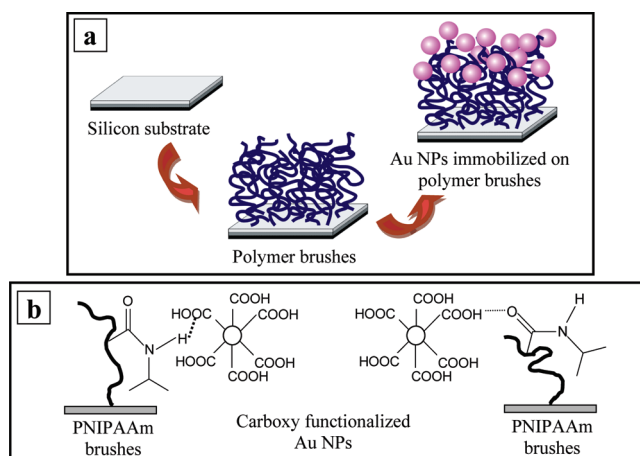
- (1) For recent reviews on nanoparticles, see: (a) Kotov, N. A. Layer-by-layer Assembly of Nanoparticles and Nanocolloids: Inter-molecular Interactions, Structure, and Material Perspectives. In *Multilayer Thin Films*; Decher, G., Schlenoff, J. B., Eds.; Wiley-VCH: Weinheim, 2003, pp 207–269. (b) Burda, C.; Chen, X.; Narayanan, R.; El-Sayed, M. A. *Chem. Rev.* **2005**, *105*(4), 1025.
- (2) Yonezawa, T.; Toshima, N. Polymer-stabilized Metal Nanoparticles. In *Advanced Functional Molecules and Polymers*; Nalwa, H. S., Ed.; Gordon and Breach: London, U.K., 2001, pp 65–86.
- (3) Ulman, A. *Chem. Rev.* **1996**, *96*, 1533.
- (4) (a) Gupta, S.; Agrawal, M.; Uhlmann, P.; Simon, F.; Oertel, U.; Stamm, M. *Macromolecules* **2008**, *41*, 8152. (b) Gupta, S.; Uhlmann, P.; Agrawal, M.; Lesnyak, V.; Gaponik, N.; Simon, F.; Stamm, M.; Eychmüller, A. *J. Mater. Chem.* **2008**, *18*, 214.
- (5) Scott, R. W. J.; Wilson, O. M.; Crooks, R. M. *J. Phys. Chem. B* **2005**, *109*, 692.
- (6) (a) Agrawal, M.; Pich, A.; Zafeiropoulos, N. E.; Gupta, S.; Pionteck, J.; Simon, F.; Stamm, M. *Chem. Mater.* **2007**, *19*, 1845. (b) Agrawal, M.; Pich, A.; Gupta, S.; Zafeiropoulos, N. E.; Simon, P.; Stamm, M. *Langmuir* **2008**, *24*, 1013.

- (7) Agrawal, M.; Pich, A.; Gupta, S.; Zafeiropoulos, N. E.; Rubio Retama, J.; Simon, F.; Stamm, M. *J. Mater. Chem.* **2008**, *18*, 2581.
- (8) Suzuki, D.; Kawaguchi, H. *Langmuir* **2005**, *21*, 8175.
- (9) Ionov, L.; Sidorenko, A.; Stamm, M. *Macromolecules* **2004**, *37*, 7421.
- (10) (a) Gupta, S.; Uhlmann, P.; Agrawal, M.; Chapuis, S.; Oertel, U.; Stamm, M. *Macromolecules* **2008**, *41*, 2874. (b) Mei, Y.; Sharma, G.; Lu, Y.; Drechsler, M.; Ballauff, M.; Irrgang, T. *Langmuir* **2005**, *21*, 12229. (c) Sharma, G.; Ballauff, M. *Macromol. Rapid Commun.* **2004**, *25*, 547.
- (11) (a) Ionov, L.; Sapra, S.; Synytska, A.; Rogach, A. L.; Stamm, M.; Diez, S. *Adv. Mater.* **2006**, *18*, 1453. (b) Liu, Z.; Pappacena, K.; Cerise, J.; Kim, J.; Durning, C. J.; O'Shaughnessy, B.; Levicky, R. *Nano Lett.* **2002**, *2*, 219.
- (12) (a) Daniel, M. C.; Astruc, D. *Chem. Rev.* **2004**, *104*, 293. (b) Yu, A.; Liang, Z.; Cho, J.; Caruso, F. *Nano Lett.* **2003**, *3*, 1203.

been made for the immobilization of Au NPs on macroscopic surfaces in order to improve the accessibility of their unusual optical properties. In comparison to the stabilization with gels or other 3-D matrixes, one can access a relatively higher surface area of the NPs by means of their immobilization over macroscopic surfaces, as in the previous case NPs remain partly or wholly inside the gels.<sup>13</sup> In addition, removal of the NPs from reaction media after the catalytic process is easier in the later case. For example, Resch et al.<sup>14</sup> reported immobilization of Au NPs on silicon dioxide surfaces by embedding them in octadecylsiloxane (ODS) and SiO<sub>2</sub> layers. In another study, Musick et al.<sup>15</sup> described self-assembly of colloidal Au NPs on an underlined substrate by exploiting the bifunctionalized organic cross-linkers. Caruso et al.<sup>12b</sup> reported fabrication of dense Au NP films by infiltrating 4-(dimethylamino) pyridine-stabilized Au NPs into polyelectrolyte multilayers preassembled on indium tin oxide (ITO) electrodes. Yamanoi et al.<sup>16</sup> explored synthesis of a series of thiol-stabilized Au NPs and their covalent immobilization on silicon substrates. Previously reported pioneering works on the immobilization of Au NPs on macroscopic surfaces are very interesting, but unfortunately, many of them have been reported to be accompanied by some disadvantages such as (1) agglomeration of adsorbed NPs on surfaces, (2) incomplete coverage of surfaces with NPs, (3) weak or reversible bonding of NPs to adhesion promoters/surface, and (4) multistep time-consuming processes to achieve multilayered adsorption of NPs.

Herein, we report on an easy and facile approach to the immobilization of Au NPs on macroscopic surfaces by exploiting chemically grafted and well-defined poly(*N*-isopropyl acrylamide) (PNIPAAm) brushes as surface modifiers. The employed protocol involves grafting of end functionalized PNIPAAm chains on an underlined substrate in brush conformation followed by immobilization of the preformed and carboxyl-functionalized Au NPs on PNIPAAm brushes. The constraint of one end attachment of PNIPAAm chains in brush conformation controls the distribution of NPs on the surface as recently reported by Liu et al.<sup>11b</sup> The schematic presentation of the proposed approach is shown in Scheme 1a. We speculate that the hydrogen bonding between amide groups of PNIPAAm chains and Carboxyl groups present at the surface of Au NPs acts as the driving force for fabrication of these nanoassemblies (as shown in Scheme 1b). We found that employed approach resulted into a homogeneous, dense, and completely covered macroscopic surface with Au NPs. In addition, we demonstrated the application of resulting PNIPAAm–Au nanoassemblies in the fabrication of temperature nanosensors on the

**Scheme 1.** (a) Schematic Presentation of the Immobilization of Au NPs onto the PNIPAAm Brushes and (b) Hydrogen Bonding between Carboxyl Groups Present on the Surface of Au NPs and Amide Groups of PNIPAAm Brushes



account of the temperature sensitivity of polymer brushes and tunable optical properties of immobilized Au NPs.

## Experimental Section

**Materials.** Hydrogen tetrachloroaurate (III) (HAuCl<sub>4</sub>·4H<sub>2</sub>O), tetraoctylammonium bromide (TOAB), 11-mercaptopundecanoic acid (MUA), and sodium borohydride all were purchased from Aldrich and used without additional purification. Carboxyl terminated poly(*N*-isopropyl acrylamide) ( $M_n = 47600 \text{ g mol}^{-1}$ ) and polyglycidyl methacrylate (PGMA) ( $M_n = 17500 \text{ g mol}^{-1}$ ) were purchased from Polymer Source, Inc. and used as received. Highly polished single-crystal silicon wafers of {100} orientation with ca. 1.5 nm thick native silicon oxide layers were purchased from Semiconductor Processing Co. and used as substrates. Dichloromethane (DCM), chloroform, toluene, and ethanol were dried using standard methods before use. Millipore water was employed throughout the experiments.

**Characterization Methods.** The thicknesses of the grafted polymer brushes were measured at  $\lambda = 632 \text{ nm}$  and an incidence angle of  $70^\circ$  with a SENTECH SE-402 scanning microfocus ellipsometer equipped with an *XY*-positioning table for mapping of the sample surface. The measurements were performed for each sample after each step of the modification to use the measurements of the previous step as a reference for the simulation of ellipsometric data.<sup>17</sup> The refractive indices used for the calculations were 3.858-i0.018, 1.4598, 1.525, and 1.499 for silicon substrate, native silica layer, PGMA layer, and PNIPAAm brushes, respectively. X-ray photoelectron spectroscopy (XPS) experiments were performed with an AXISULTRA spectrometer (Kratos Analytical, U.K.) equipped with a monochromized Al K $\alpha$  X-ray source of 300 W at 20 mA. The survey spectra and high-resolution spectra were obtained at an analyzer's pass energy set value of 160 and 20 eV, respectively. All spectra were charge compensated using the C<sub>1s</sub>H<sub>1s</sub> component peak of the C 1s spectra at BE (binding energy) 285.00 eV as the reference peak.<sup>18</sup> To determine elemental ratios, normalized

- (13) (a) Bharathi, S.; Lev, O. *Chem. Commun.* **1997**, 2303. (b) Matsuoka, J.; Mizutani, R.; Kaneko, S.; Nasu, H.; Kamiya, K.; Kadono, K.; Sakaguchi, T.; Miya, M. *J. Ceram. Soc. Jpn.* **1993**, 101, 53.  
 (14) Resch, R.; Meltzer, S.; Vallant, T.; Hoffmann, H.; Koel, B. E.; Madhukar, A.; Requicha, A. A. G.; Will, P. *Langmuir* **2001**, 17, 5666.  
 (15) Musick, M. D.; Pena, D. J.; Botsko, S. L.; McEvoy, T. M.; Richardson, J. N.; Natan, M. J. *Langmuir* **1999**, 15, 844.  
 (16) Yamanoi, Y.; Yonezawa, T.; Shirahata, N.; Nishihara, H. *Langmuir* **2004**, 20, 1054.

- (17) Minko, S.; Patil, S.; Datsyuk, V.; Simon, F.; Eichhorn, K. J.; Motornov, M.; Usov, D.; Tokarev, I.; Stamm, M. *Langmuir* **2002**, 18, 289.  
 (18) Beamson, G.; Briggs, D. *High resolution XPS of organic polymers*; The Scienta ESCA 300 Database; J. Wiley & Sons: Chichester, New York, Brisbane, Toronto, Singapore, ISBN 0-471-93592-1, 1992, p 278.

peak areas ( $\phi$ ) were calculated from peak areas ( $A$ ) of survey spectra, respecting experimentally determined sensitivity factors and the spectrometer's transmission function using following equation:

$$\phi = \frac{A}{\text{RSF} \times \text{Tx}} \quad (1)$$

where RSF is the respecting sensitivity factor<sup>19</sup> and Tx is the spectrometer's transmission function. The advancing water contact angle was measured using "DSA-10" Krüss equipment with an accuracy of 0.5°. UV-vis spectra were recorded with a Cary 50 spectrophotometer (Varian). Atomic force microscopy (AFM) studies were performed with a Dimension 3100 (Digital Instruments, Inc., Santa Barbara, CA) microscope. Tapping mode was used to map the film morphology at ambient conditions. Transmission electron microscopy (TEM) images were recorded on Zeiss Omega 912 microscope at an accelerating voltage of 200 kV.

**Preparation of Polymer Brushes.** PNIPAAm brushes were grown on silicon substrates by exploiting the "grafting to" method.<sup>20</sup> Silicon wafers (2 cm × 1 cm) were used as underlined substrates, which were cleaned with dichloromethane in an ultrasonic bath for 45 (15 × 3) min prior to their further modification. Subsequently, these substrates were stirred by means of an in-house fabricated wafer holder in a 1:1 mixture of 29% ammonium hydroxide and 30% hydrogen peroxide (*WARNING: This solution is extremely corrosive and should not be stored in tightly sealed containers due to evolution of gas*) for 1.5 h and then rinsed several times with Millipore water. A thin layer of PGMA (ca. 2 nm) was deposited on the substrate by spin-coating from a 0.02 w/w % solution in chloroform and annealed at 110 °C for 10 min. Subsequently, a thin film of carboxyl-functionalized PNIPAAm (1.6 w/w % solution in chloroform) was spin-coated and annealed at 170 °C for 16 h in a vacuum oven. Finally, PNIPAAm modified surfaces were cleaned by means of Soxhlet extraction in chloroform for 4 h.

**Preparation of Gold Nanoparticles.** Au NPs were synthesized by borohydride reduction of chlorauric acid as described elsewhere.<sup>4a</sup> In a typical process, 50 mL of aqueous solution of HAuCl<sub>4</sub>·4H<sub>2</sub>O (15 mM) was mixed with 328 mg of TOAB (0.6 mmol) dissolved in 100 mL of toluene, and subsequently, the resulting mixture was added to a solution of 32.75 mg of MUA (0.15 mmol) in 25 mL of toluene dropwise under vigorous stirring at 23 °C. A freshly prepared 25 mL aqueous solution of 0.30 M NaBH<sub>4</sub> was added into the reaction media, and the resulting mixture was allowed to stir for another 1 h. The organic phase was separated, washed with distilled water, and concentrated to dryness under reduced pressure. Resulting black solid was heat treated at 155 °C at the heating rate of 2 K min<sup>-1</sup> for 30 min. This heat-treated product was dissolved in toluene and mixed with chloroform to remove the excess of TOAB and MUA. Finally, Au NPs were separated from the solution by means of ultracentrifugation.

**Immobilization of Nanoparticles on PNIPAAm Brushes.** Au NPs were immobilized on PNIPAAm brushes modified silicon substrates by incubating the samples into their 1 mM solution in toluene, overnight. Non- or weakly adsorbed particles were removed by repetitive rinsing of the samples with toluene.

## Results and Discussion

Well-defined and homogeneously distributed end functionalized PNIPAAm brushes were prepared on a silicon substrate by exploiting the well-known "grafting to" approach.<sup>9,20</sup> The process involves chemisorption of the PGMA anchoring layer on the silicon substrate followed by the chemical grafting of carboxyl-functionalized PNIPAAm chains. It is well-known from literature that PGMA can be used as a universal anchoring layer for grafting of a variety of polymer brushes on a wide range of underlining substrates.<sup>21</sup> Dry thickness and contact angle of polymer brushes have been measured as 18 nm and 70 ± 2.5°, respectively. Grafting density of the obtained PNIPAAm brushes has been estimated as 0.15 chains/nm<sup>2</sup> by  $\sigma = 1/d_g^2$ . Here,  $d_g$  is the distance between two grafting sites which was derived from  $d_g = M_n^{1/2} (N_A \cdot d\rho)^{-1/2}$  as 2.58 nm, where  $M_n$  is number average molecular weight of polymer chains,  $N_A$  is Avogadro's number,  $\rho$  is polymer density for PNIPAAm (~1.0 g/cm<sup>3</sup>), and  $d$  is dry state thickness of PNIPAAm brushes.<sup>22</sup>

Au NPs with particle sizes of 5 to 6 nm have been synthesized and modified with a shell of 11-mercaptopundecanoic acid as described elsewhere.<sup>23</sup> The immobilization of Au NPs on polymer brushes has been realized by exploiting the physical interaction (hydrogen bonding) between amide functionalities of PNIPAAm chains and surface functionalities (–COOH groups) of Au NPs. Supporting Information 1a shows a TEM image of the Au NPs revealing their size in the range of 5 to 6 nm. It is well-known from the literature that modulation in size and proximity of the Au NPs leads to the shift in their surface plasmon resonance (SPR) band position. In order to achieve this variation in optical properties for nano-sensor applications, Au NPs should be <20 nm in diameter with a narrow particle size distribution.<sup>24</sup> Supporting Information 1b shows a UV-vis spectrum of these Au NPs, indicating a strong SPR band at the characteristic position 520 nm. Overnight incubation of the samples into the Au NPs (dispersed in toluene) resulted into the immobilization of NPs onto the PNIPAAm brushes. The presence of the long alkyl chains in the 11-mercaptopundecanoic acid shell of Au NPs render them hydrophobic to disperse into the toluene by means of the hydrophobic–hydrophobic interactions. This fine dispersion of the Au NPs into the incubated toluene solution resulted into their homogeneous distribution onto the PNIPAAm brushes. Obtained Au immobilized PNIPAAm brushes have been thoroughly characterized with a variety of analytical tools. Samples were cleaned with toluene before

(19) Experimentally determined for our spectrometer KRATOS AXIS ULTRA.

(20) Ionov, L.; Stamm, M.; Diez, S. *Nano Lett.* **2006**, *6*, 1822.

(21) Luzinov, I.; Iyer, K. S.; Klep, V.; Zdyrko, B.; Draper, J.; Liu, Y. *Polym. Prepr.* **2003**, *44*(1), 437.

(22) Zdyrko, B.; Klep, V.; Luzinov, I. *Langmuir* **2003**, *19*, 10179.

(23) Matsui, J.; Akamatsu, K.; Nishiguchi, S.; Miyoshi, D.; Nawafune, H.; Tamaki, K.; Sugimoto, N. *Anal. Chem.* **2004**, *76*, 1310.

(24) (a) Kreibitz, U.; Vollmer, M. *Optical Properties of Metal Clusters*; Springer-Verlag: Berlin, 1995. (b) Schmid, G., Ed. *Clusters and Colloids, from Theory to Applications*; VCH: New York, 1994. (c) Alivisatos, A. P. *J. Phys. Chem.* **1996**, *100*, 13226. (d) Fendler, J. H.; Meldrum, F. C. *Adv. Mater.* **1995**, *7*, 607.



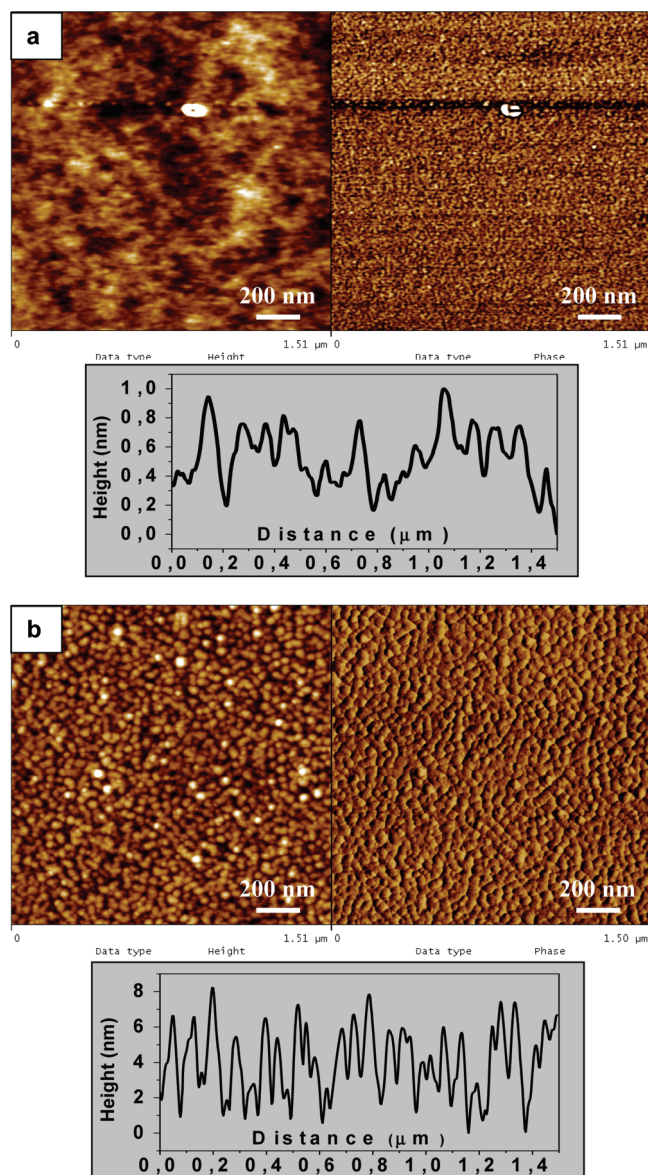


**Figure 1.** AFM height (left) and phase (right) images ( $1.5 \times 1.5 \mu\text{m}$ ) and height profiles (below) of PNIPAAm brushes (a) before and (b) after immobilization of Au NPs.

analyzing them to ensure the complete removal of the nonimmobilized Au NPs.

Figure 1 illustrates topographic and phase AFM images of PNIPAAm brushes before and after the immobilization of Au NPs. One can observe that the morphology of polymer brushes has turned from “carpetlike” to “pebbled one” after the immobilization process, strongly confirming the presence of a dense layer of Au NPs onto the PNIPAAm brushes. It can be further evidenced by the height profiles of topographic AFM images of polymer brushes shown in Figure 1, which reveal a significant change in root-mean-square (rms) roughness of brushes from 0.4 to 2.2 nm after the immobilization of Au NPs. In order to rule out the fact that apparent pebbled morphology of polymer brushes, appeared after the immobilization process, is induced by their overnight incubation in toluene; a control experiment has been performed. For this purpose, bare PNIPAAm brushes have

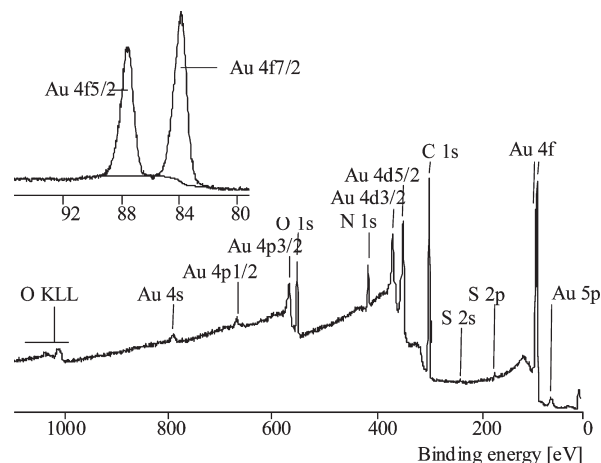


**Figure 2.** XPS wide-scan spectrum of PNIPAAm brushes immobilized with Au NPs. Inset shows Au 4f core level spectra of the sample revealing the signature doublet of Au 4f.

been incubated into the toluene overnight and analyzed by AFM. A comparison of the AFM images of toluene treated bare PNIPAAm brushes (shown in Supporting Information 2) and Figure 1a clearly reveals that overnight incubation of the samples in toluene hardly affects their surface morphology, and hence, it can be concluded that apparent pebbled structures in Figure 1b are the sites of Au NPs. It is also noteworthy that immobilized particles are spherical in shape and form a homogeneously distributed and closely packed layer on macroscopic surfaces. It should be noted that AFM tip convolution effects magnify the observed particle size in the range of 20–30 nm.<sup>12b</sup> Surface coverage of Au NPs on polymer brushes was estimated to be 22% by  $\varphi = 100\% \cdot N \cdot \pi \cdot d^2 / 4A$  where  $d$  is the diameter of the nanocrystals and  $N$  is the number of NPs detected per area  $A$ . The number of NPs per area of the sample was counted by zooming a part of the AFM image. A close inspection of these AFM images reveals that the described protocol is able to offer a homogeneous immobilization of Au NPs on macroscopic surfaces. The preparation of thin films with a high density of metal NPs is often desired for catalysis and electronics applications.<sup>25</sup>

The presence of Au NPs on polymer brushes has been further evidenced by XPS analysis. Figure 2 shows a wide scan spectrum of PNIPAAm brushes immobilized with Au NPs. A comparison of this spectra with that of bare PNIPAAm brushes (shown in Supporting Information 3) reveals presence of the characteristic “Au” signals at relevant binding energies (Au 4f  $\sim 84$  eV), suggesting the immobilization of Au NPs on polymer brushes.<sup>26</sup> In addition, the inset in Figure 2 represents the XPS signature of the Au 4f doublet for the PNIPAAm–Au nano-assemblies. The binding energies of the doublet for Au 4f<sub>7/2</sub> and 4f<sub>5/2</sub> have been found as 83.2 and 86.9 eV, respectively, which are consistent with the Au<sup>0</sup> oxidation state. In addition, it should also be noted that absence of a peak

(25) Niemeyer, C. M. *Angew. Chem., Int. Ed.* **2001**, *40*, 4128.

(26) Moulder, J. F.; Stickle, W. F.; Sobol, P. E.; Bombier, K. D. In *Handbook of X-ray Photoelectron Spectroscopy*; Chastian, J., Ed.; Perkin-Elmer Corp.: Waltham, MA, 182.

near 84.9 eV rules out the presence of any features due to the  $\text{Au}^+$  oxidation state.<sup>27</sup> The atomic concentration of the Au on the investigated substrates has been found as approximately 3.69% by XPS analysis. It is believed that most of the NPs are immobilized on the upper part of the polymer brushes. Owing to the steric hindrance caused by the polymer chains, particles do not penetrate significantly into the brush layer.<sup>4a</sup>

In order to investigate the optical properties of the immobilized Au NPs, samples have been analyzed by UV–vis spectroscopy and results are shown in Figure 3a. These data reveal no absorption band for the bare PNIPAAm brushes (black curve), while a symmetric absorption band at 566 nm for the Au immobilized PNIPAAm brushes in a dry state (blue curve) suggests the presence of Au NPs on the polymer brushes.<sup>28,29</sup> It is worth mentioning here that absence of the optical signature at a higher wavelength ( $> 600$  nm) excludes the possibilities of significant aggregation of immobilized Au NPs on the PNIPAAm brushes.<sup>30,31</sup>

It has been realized that external stimuli induced modulation in the thickness of polymer brushes affords great opportunities for a wide range of nanotechnological areas and opens up a new avenue in nanosensor applications.<sup>4a,11a</sup> In the first set of the experiments, we investigated modulation in optical properties of Au NPs immobilized on PNIPAAm brushes with the variation in surrounding media from air to water, and results are shown in Figure 3a. One can observe that the SPR peak of immobilized Au NPs has shifted from 566 nm in the dry state (blue curve) to 547 nm in aqueous media at pH 7 and 23 °C (pink curve). In addition, the absorption band has been found to be significantly broader in the previous case than the later one. These observations can be attributed to the fact that PNIPAAm brushes swell in water at room temperature leading to the increase in interparticle distance of immobilized NPs. It is well-known from literature that an increase in interparticle distance of optically active NPs leads to the blue shift in their peak positions.<sup>32,33</sup> On the other hand, particles are relatively closer in the dry state as PNIPAAm chains are collapsed and a red shift in band position is observed. It should be noted that modulation in absorption band positions with the variation in surrounding media has been found nearly reversible. We have observed the same phenomena with the fabrication of pH and solvent nanosensors in our previous studies.<sup>4a,10a</sup>

Underlying the LCST (lower critical solution temperature) behavior of PNIPAAm,<sup>34</sup> we also examined

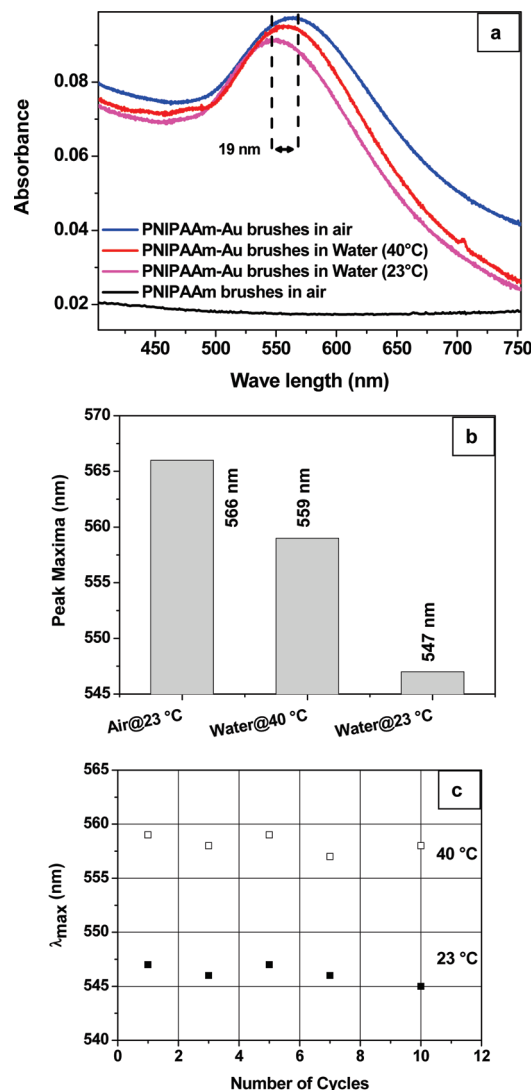


**Figure 3.** (a) UV–vis spectra of PNIPAAm brushes and PNIPAAm–Au brushes taken in air and aqueous media. (b) Variation in the position of the surface plasmon resonance peak of immobilized Au NPs with the change in surrounding media from air to water and temperature of aqueous media. (c) SPR band positions of Au NPs below and above the LCST of the PNIPAAm brushes after a number of heating and cooling cycles.

the variation in optical properties of PNIPAAm–Au brushes as a function of the temperature in aqueous media. When samples have been immersed in the water and heated from 23 to 40 °C (above the LCST), the SPR peak has been observed to red shift from 547 nm (pink curve in Figure 3a) to 559 nm (red curve in Figure 3a). In addition, the peak area has also been found to slightly increase, indicating the agglomeration of immobilized Au NPs with an increase in temperature.

A schematic presentation of the swelling–deswelling behavior of polymer brushes with the change in temperature and respective variation in peak position of immobilized Au NPs are shown in Figure 4a. This modulation in optical properties of Au NPs can be attributed to the temperature induced collapse of PNIPAAm brushes at 40 °C. As illustrated in Figure 4b, PNIPAAm chains interact with water molecules by means of hydrogen bonding below LCST and, hence, remain in the swollen

- (27) Brust, M.; Walker, M.; Bethell, D.; Schiffrin, D. J.; Whyman, R. *J. Chem. Soc., Chem. Commun.* **1994**, 801.
- (28) Elghanian, R.; Storhoff, J. J.; Mucic, R. C.; Letsinger, R. L.; Mirkin, C. A. *Science* **1997**, 277, 1078.
- (29) Storhoff, J. J.; Lazarides, A. A.; Mucic, R. C.; Mirkin, C. A.; Letsinger, R. L.; Schatz, G. C. *J. Am. Chem. Soc.* **2000**, 122, 4640.
- (30) Weisbecker, C. S.; Merritt, M. V.; Whitesides, G. M. *Langmuir* **1996**, 12, 3763.
- (31) Nath, N.; Chilkoti, A. *J. Am. Chem. Soc.* **2001**, 123, 8197.
- (32) Takeuchi, Y.; Ida, T.; Kimura, K. *Surf. Rev. Lett.* **1996**, 3, 1205.
- (33) Kreibitz, U.; Genzel, L. *Surf. Sci.* **1985**, 156, 678.
- (34) Schild, H. G. *Prog. Polym. Sci.* **1992**, 17, 163.

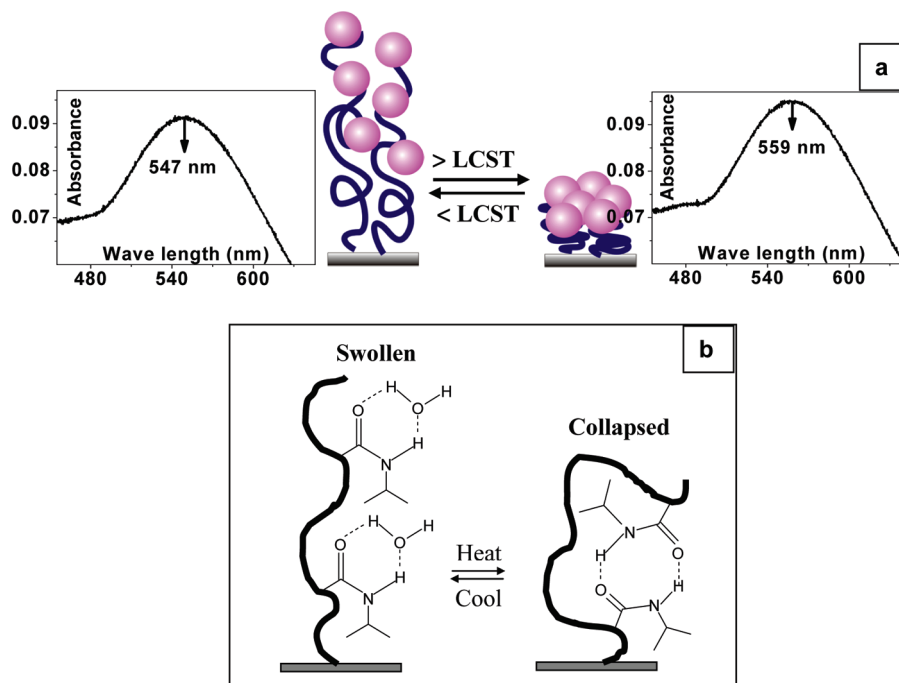


**Figure 4.** (a) Schematic illustration of the swelling–deswelling of PNIPAAm–Au brushes in water below and above LCST and modulation in the optical properties of the immobilized Au NPs. (b) Variation in the nature of the hydrogen bonding in PNIPAAm chains with temperature.

state. As the temperature is increased above the LCST, they collapse and form the intramolecular hydrogen bonding. A decrease in interparticle distance caused by the collapse of polymer chains led to the red shift in the SPR peak. A comparison of the UV–vis spectrum of PNIPAAm–Au brushes in the dry state with the one taken in the collapsed state in water at 40 °C reveals that Au NPs are much closer in the previous case as compared to the later one. It can be attributed to the relatively higher mobility of the grafted PNIPAAm chains in water as compared to the dry state. As shown in Figure 3c, the SPR band positions of immobilized Au NPs have been found nearly reversible with the modulation of the temperature. It is worth mentioning here that the apparent shift of 12 nm in the absorption band position of the immobilized Au NPs with the temperature is significantly higher than the one reported in literature for PNIPAAm embedded Au NPs.<sup>35</sup> It is needless to mention that the extent of the shift in SPR band position manifests the sensitivity of the nanosensors. It can be attributed to significantly smaller size (5 to 6 nm) of the immobilized Au NPs and the design of the nanosensors, which allows the modulation in interparticle distance of the Au NPs with the swelling and deswelling of PNIPAAm brushes.

Figure 3b compares the SPR band positions of PNIPAAm–Au nanoassemblies with the variation in surrounding media and temperature. These observations indicate that fabricated nanosensors can be used to sense the nature of the surrounding media such as in microfluidic devices from dry to the wet state and vice versa, as well as temperature in aqueous media. However, we have to admit that fabricated sensors are applicable to sense

the temperature only below and above the LCST of the PNIPAAm. Nevertheless, one can exploit the same methodology in biological applications for reversible and temperature induced switching of bioactive agents by modifying the surfaces of the interests with PNIPAAm brushes.

## Conclusions

In summary, we have demonstrated a simple and facile approach to the immobilization of Au NPs onto the macroscopic surfaces by exploiting the temperature responsive polymer brushes as adhesion promoters. Resulting PNIPAAm–Au nanoassemblies have been used for the fabrication of temperature nanosensors by exploiting the temperature induced swelling–deswelling of polymer brushes and tunable optical properties of immobilized Au NPs. In addition to demonstrated sensing application, we believe that immobilized NPs can offer the large surface area as compared to the bulk ones and, thus, fabricated nanoassemblies can effectively be used as the catalyst in photocatalytic reactions. The employed approach is versatile in nature and can be applied to modify various macroscopic surfaces via immobilization of different types of NPs.

**Acknowledgment.** The authors are thankful to Mr. Axel Mensch and Dr. Ulrich Oertel for helping with TEM and UV–vis analyses.

**Supporting Information Available:** TEM image and UV–vis spectrum of Au NPs, AFM images of solvent treated PNIPAAm brushes, XPS spectra of PNIPAAm brushes (PDF). This material is available free of charge via the Internet at <http://pubs.acs.org>.

(35) Mitsuishi, M.; Koishikawa, Y.; Tanaka, H.; Sato, E.; Mikayama, T.; Matsui, J.; Miyashita, T. *Langmuir* **2007**, *23*, 7472.